

CURRENT STATUS OF DENSE CERMET MEMBRANES FOR HYDROGEN
SEPARATION*

U. (Balu) Balachandran, T. H. Lee, S. Wang, C. Zuo and
S. E. Dorris

Energy Technology Division
Argonne National Laboratory
Argonne, IL 60439-4838

K. S. Rothenberger
National Energy Technology Laboratory
Pittsburgh, PA 15236-0940

June 2003

Paper to be presented at the 20th Annual International Pittsburgh Coal Conference,
Pittsburgh, PA, Sept. 15-19, 2003.

* Work supported by U.S. Department of Energy, Office of Fossil Energy, National Energy
Technology Laboratory's Gasification Technologies Program, under Contract W-31-109-Eng-38.

CURRENT STATUS OF DENSE CERMET MEMBRANES FOR HYDROGEN SEPARATION*

U. (Balu) Balachandran (balu@anl.gov; 630-252-4250)
T. H. Lee (thlee@anl.gov; 630-252-5374)
S. Wang (shwang@anl.gov; 630-252-4193)
C. Zuo (zuo@anl.gov; 630-252-5115)
S. E. Dorris (dorris@anl.gov; 630-252-5084)

Energy Technology Division
Argonne National Laboratory
Argonne, IL 60439-4838

K. S. Rothenberger (kurt.rothenberger@netl.doe.gov; 412-386-6082)
National Energy Technology Laboratory
Pittsburgh, PA 15236-0940

ABSTRACT

Argonne National Laboratory (ANL) and the National Energy Technology Laboratory (NETL) are developing dense membranes for separating hydrogen from mixed gases, particularly product streams generated during coal gasification, methane partial-oxidation, and water-gas shift reactions. Hydrogen separation with these membranes is nongalvanic, i.e., it does not use electrodes or an external power supply to drive the separation, and hydrogen selectivity is nearly 100% because the membranes contain no interconnected porosity.

Novel cermet membranes (i.e., ceramic-metal composites) have been developed to separate hydrogen from gas mixtures at high temperature and pressure. These membranes (ANL-1, -2, and -3) are classified according to the hydrogen transport properties of their metal and ceramic phases. We report results regarding the thermodynamic stability and electrical conductivity of $\text{BaZr}_{0.8-x}\text{Pr}_x\text{Y}_{0.2}\text{O}_3$ ($x \leq 0.8$), materials that are being considered as a potential ceramic matrix in ANL-1 and -2 membranes. The hydrogen flux through ANL-3e membranes is reported as a function of membrane thickness and partial pressure of hydrogen in the feed gas. The results indicate that the hydrogen flux through ANL-3e membranes is limited by bulk diffusion of hydrogen through the metal phase in the thickness range of 22-100 μm . The highest hydrogen flux for an ANL-3e membrane (19.0 cm^3 (STP)/min- cm^2) was measured with a 22- μm -thick sample at 900°C using 100% H_2 as the feed gas. This value is only slightly lower than the record flux measured with an ANL-3a membrane (20 cm^3 (STP)/min- cm^2). The hydrogen flux of ANL-3e membranes was stable for up to 120 h in atmospheres containing up to 400 ppm H_2S . While longer-term (>120 h) studies are needed, these results indicate that the membranes may be suitable for practical applications.

INTRODUCTION

Hydrogen is an attractive fuel for both the electric power and transportation industries because its entirely pollution-free combustion addresses rising concerns over global climate change. Producing abundant supplies of hydrogen from fossil and renewable resources would diversify the domestic energy supply and help to reduce dependence on foreign sources. In his 2003 State of the Union address, President Bush announced a Hydrogen Fuel Initiative to develop hydrogen production and distribution technologies for powering fuel-cell vehicles and stationary fuel-cell power sources. The goal of this initiative is to lower the cost of hydrogen enough to make fuel-cell cars cost-competitive with conventional gasoline-powered vehicles by 2010, and to advance the methods of producing hydrogen from renewable resources, nuclear energy, and coal. As part of the effort to devise cost-effective, efficient processes for producing and utilizing hydrogen, Argonne National Laboratory (ANL) and the National Energy Technology Laboratory (NETL) are developing dense, hydrogen-permeable membranes.

The goal at ANL/NETL is to develop a dense, ceramic-based membrane that is highly selective, chemically stable in corrosive environments at operating temperatures up to $\approx 900^\circ\text{C}$, and can separate hydrogen from mixed gases at commercially significant fluxes under industrially relevant operating conditions. The effort at ANL/NETL initially focused on $\text{BaCe}_{0.8}\text{Y}_{0.2}\text{O}_{3-\square}$ (BCY), a mixed proton/electron conductor whose high total electrical conductivity [1, 2] suggested that it may yield a high hydrogen flux without need for electrodes or electrical circuitry. Early results showed, however, that the electronic component of conductivity for BCY is insufficient to support a high nongalvanic hydrogen flux [3, 4]. To increase the electronic conductivity, and thereby increase the hydrogen flux, we have developed various cermet (i.e., ceramic-metal composite) membranes, in which 40-50 vol.% of a metal is dispersed in a ceramic matrix [5, 6].

The cermet membranes being developed by ANL/NETL are classified as ANL-1, -2, or -3 on the basis of the hydrogen transport properties of the metal and matrix phases. In ANL-1 membranes, a metal with low hydrogen permeability is distributed in the hydrogen-permeable matrix of BCY. ANL-2 membranes also have a matrix of hydrogen-permeable BCY, but they contain a hydrogen transport metal, i.e., a metal with high hydrogen permeability. In ANL-3 membranes, a metal with high hydrogen permeability is dispersed in a ceramic matrix of low hydrogen permeability, e.g., Al_2O_3 , ZrO_2 , or BaTiO_3 . Each membrane is identified by a number representing the class of membrane as described above and a letter indicating a specific combination of metal and matrix phases. For example, ANL-3a is an ANL-3 membrane that contains a specific metal in a matrix of Al_2O_3 , whereas ANL-3b contains a different combination of hydrogen transport metal and ceramic. A letter is not included when general comments are made about an entire class of membranes, e.g., ANL-3 membranes.

Hydrogen permeation through ANL-1a is higher than that in monolithic BCY because the metal in ANL-1a increases its electronic conductivity. Because the metal in ANL-1a has low hydrogen permeability, only a small part of the hydrogen diffuses through the metal phase. ANL-2a membranes, in which a hydrogen transport metal replaces the metal of ANL-1a, gives a still higher hydrogen flux. The metal in ANL-2a

facilitates hydrogen diffusion by increasing the electronic conductivity and by providing an alternative path for hydrogen diffusion. Although BCY and the metal phase both contribute to hydrogen permeation through ANL-2 membranes, most of the hydrogen diffuses through the metal, while only a small amount diffuses through BCY [7].

Because BCY contributes relatively little to the hydrogen flux through ANL-2 membranes, has poor mechanical properties, and is chemically unstable under some conditions of interest [8], we began investigating possible alternatives. BaPrO₃ and BaZrO₃ are promising: BaPrO₃ is reported to have a very high conductivity [9-11] but rather poor chemical stability, whereas BaZrO₃ is reported to have excellent stability but relatively low conductivity (especially electronic conductivity) [9, 12, 13]. In an attempt to balance the high conductivity of BaPrO₃-based materials with the good stability of BaZrO₃-based materials, we are investigating intermediate compositions given by the formula BaZr_{0.8-x}Pr_xY_{0.2}O₃. In this paper, we report initial analytical results of these materials.

We also studied ANL-3 membranes, which contain a hydrogen transport metal in a thermodynamically stable ceramic matrix with superior mechanical properties, e.g., Al₂O₃ or ZrO₂. These membranes have high hydrogen permeability, improved strength, and greater chemical stability compared to ANL-2 membranes. While ANL-3a membranes have attained the highest hydrogen flux to date (20 cm³(STP)/min-cm²) for an ANL/NETL membrane, they require sintering at relatively high temperature to eliminate interconnected porosity. In some cases, sintering at high temperature causes the metal phase to exude from the membrane, which also creates interconnected porosity. To lower the sintering temperature and eliminate interconnected porosity, we developed ANL-3e membranes, which contain the same hydrogen transport metal (50 vol.%) as ANL-3a membranes but use a ceramic matrix that densifies at lower temperatures. We report here hydrogen flux measurements for ANL-3e membranes as a function of membrane thickness. Also, because hydrogen separation membranes are expected to contact gas streams in which H₂S is present, the stability of membranes in H₂S-containing gas mixtures is an important issue. We report here the hydrogen flux of ANL-3e membranes versus time during exposure to feed gas containing up to ≈3000 ppm H₂S.

EXPERIMENTAL

Compositions in the system BaZr_{0.8-x}Pr_xY_{0.2}O₃ were prepared by solid-state reaction using BaCO₃, ZrO₂, Pr₂O₃, and Y₂O₃ as starting materials. Precursor powder mixtures were calcined twice at 1000-1100°C in air with intermittent grinding. The resultant powders were analyzed by X-ray diffraction (Scintag) to assure their phase-purity, then were ground and uniaxially pressed into disks. The sintering temperature for the disks varied monotonically with composition. BaPr_{0.8}Y_{0.2}O₃ (x = 0.8) was prepared by sintering 12 h at 1500°C in air, and reached a density of ≈94% of theoretical (6.32 g/cm³). BaZr_{0.8}Y_{0.2}O₃ (x = 0.0) required a much higher sintering temperature; its final density was only ≈90% of theoretical (6.20 g/cm³) after sintering for 12 h at 1650°C in air. Conductivity was measured in air and 4% H₂/balance N₂ by impedance analysis (Solartron SI 1260).

The powder mixture used to fabricate ANL-3e membranes was prepared by mechanically mixing 50 vol.% of hydrogen transport metal with a ceramic powder that can be sintered relatively easily. The powder mixture was uniaxially pressed into disks that were sintered at 1400°C for 5 h in ambient air. For permeation tests, both sides of the disks were polished using 600-grit SiC paper to obtain the desired thickness and produce faces that were flat and parallel to one another. The hydrogen permeation rate (i.e., hydrogen flux) was measured by a procedure described elsewhere [14]. The stability of ANL-3e membranes in H₂S-containing atmospheres was determined by measuring the hydrogen flux versus time in atmospheres with progressively higher H₂S concentrations. Gas mixtures for these tests were prepared using mass flow controllers to blend ultra high purity (UHP) He with H₂ that contained a known H₂S concentration. The compositions of the gas mixtures and the H₂S-containing gas used to prepare them are given in Table 1.

Table 1. Compositions of gas mixtures used to test stability of ANL-3e membranes in H₂S-containing atmospheres and components used to prepare the mixtures.

<u>Composition of Gas Mixture</u>	<u>Gases Used to Prepare Mixture</u>
51 ppm H ₂ S/19.2% H ₂ /Balance He	250 ppm H ₂ S/balance H ₂ & UHP He
97 ppm H ₂ S/19.4% H ₂ /Balance He	500 ppm H ₂ S/balance H ₂ & UHP He
400 ppm H ₂ S/79.8% H ₂ /Balance He	500 ppm H ₂ S/balance H ₂ & UHP He
2922 ppm H ₂ S/19.2% H ₂ /Balance He	1.5% H ₂ S/balance H ₂ & UHP He

RESULTS

Figure 1 shows the X-ray diffraction powder patterns for selected compositions in the BaZr_{0.8-x}Pr_xY_{0.2}O₃ system. These patterns show that compositions with x=0.0, 0.2, 0.3, 0.4, and 0.8 are all single-phase materials. As the Zr content increases, the peak positions shift to higher angles because the perovskite unit cell shrinks due to the smaller ionic radius of Zr⁴⁺ (R^{IV} = 0.72 Å) relative to Pr⁴⁺ (R^{IV} = 0.85 Å) [15].

The stability of the x = 0.0, 0.4, and 0.8 compositions was evaluated with samples that had been stored in humidified air (≈3 vol.% H₂O) for 96 h at room temperature. The x = 0.8 composition crumbled easily with handling, whereas BaZr_{0.4}Pr_{0.4}Y_{0.2}O₃ showed no such signs of poor stability. As seen in Fig. 2, the x = 0.8 composition initially showed only X-ray diffraction peaks for the BaPr_{0.8}Y_{0.2}O₃ phase, but diffraction peaks for new phases appeared after exposure to moist air. By contrast, the powder patterns for the x = 0.4 composition showed no evidence of decomposition after the exposure, indicating that the substitution of Zr has improved chemical stability with respect to BaPr_{0.8}Y_{0.2}O₃.

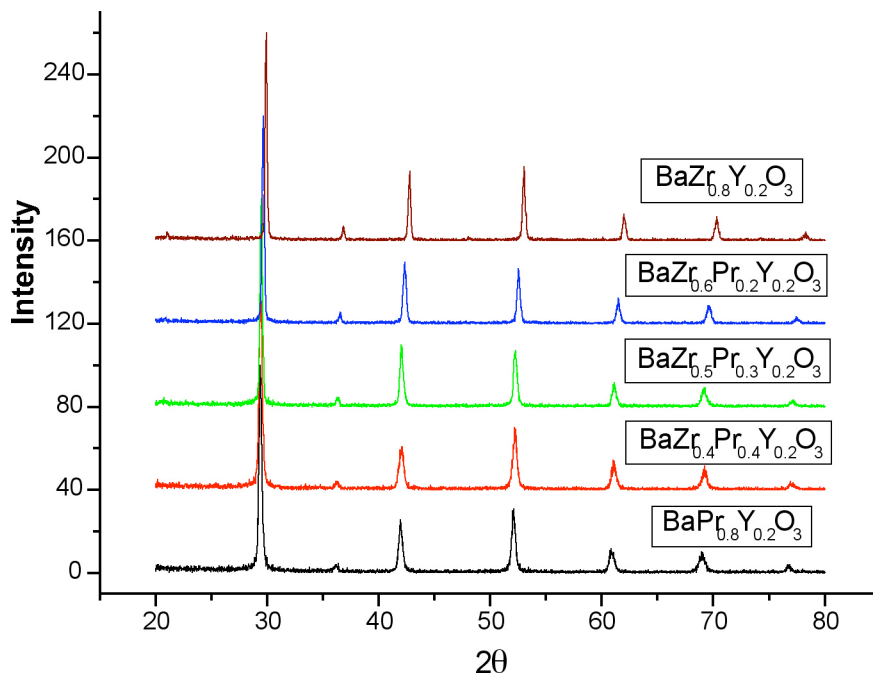


Figure 1. X-ray diffraction patterns for selected compositions in the $\text{BaZr}_{0.8-x}\text{Pr}_x\text{Y}_{0.2}\text{O}_3$ system.

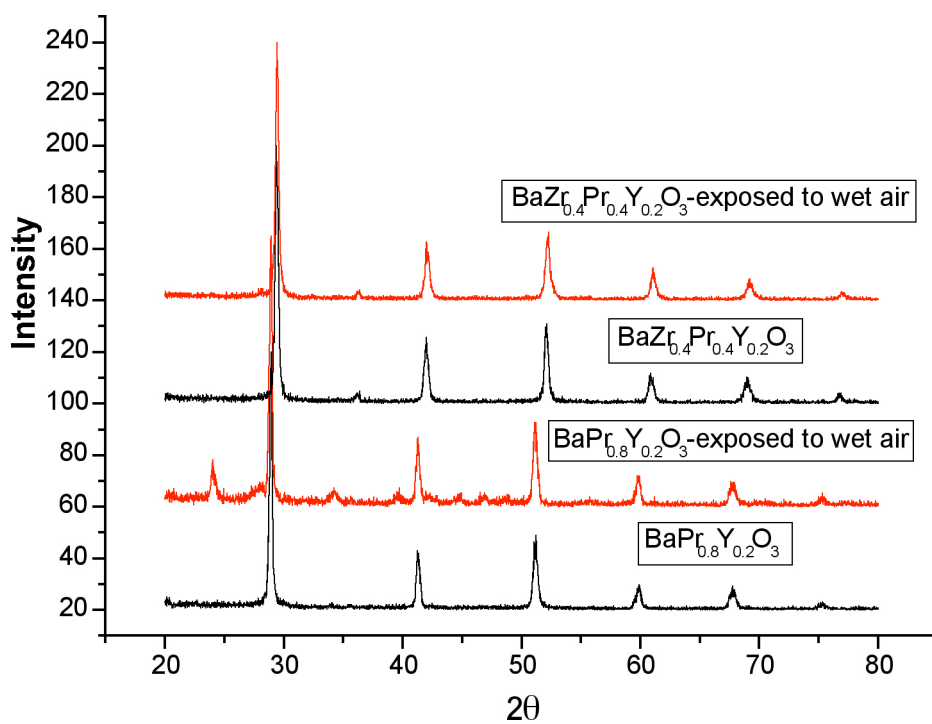


Figure 2. X-ray diffraction patterns for $\text{BaZr}_{0.4}\text{Pr}_{0.4}\text{Y}_{0.2}\text{O}_3$ and $\text{BaPr}_{0.8}\text{Y}_{0.2}\text{O}_3$ before and after exposure to humidified air (≈ 3 vol.% H_2O) at room temperature.

Figure 3 shows total conductivity data for the $x = 0.0, 0.4, \text{ and } 0.8$ compositions of $\text{BaZr}_x\text{Pr}_{0.8-x}\text{Y}_{0.2}\text{O}_3$ along with the conductivity of BCY for comparison. While the conductivity of $\text{BaPr}_{0.8}\text{Y}_{0.2}\text{O}_3$ ($x = 0.8$) is the highest and is considerably higher than that of BCY over the entire temperature range, previous studies [12-14] suggest that the conductivity of $\text{BaPr}_{0.8}\text{Y}_{0.2}\text{O}_3$ is predominantly electronic. The nature of the charge carriers needs to be determined, because this material will not be useful as a hydrogen separation membrane unless a large fraction of its conductivity is protonic. Substituting Pr for Zr to get the $\text{BaZr}_{0.4}\text{Pr}_{0.4}\text{Y}_{0.2}\text{O}_3$ composition gives a conductivity that is much higher than that of $\text{BaZr}_{0.8}\text{Y}_{0.2}\text{O}_3$. While this study is in its initial stages, preliminary results indicate that intermediate compositions ($0 < x < 0.8$) have better chemical stability than $\text{BaPr}_{0.8}\text{Y}_{0.2}\text{O}_3$ and higher conductivity than $\text{BaZr}_{0.8}\text{Y}_{0.2}\text{O}_3$. However, all samples were extremely brittle after their conductivities were measured, possibly due to their decomposition in 4% $\text{H}_2/\text{balance N}_2$. Chemical stability thus remains an important issue for these materials.

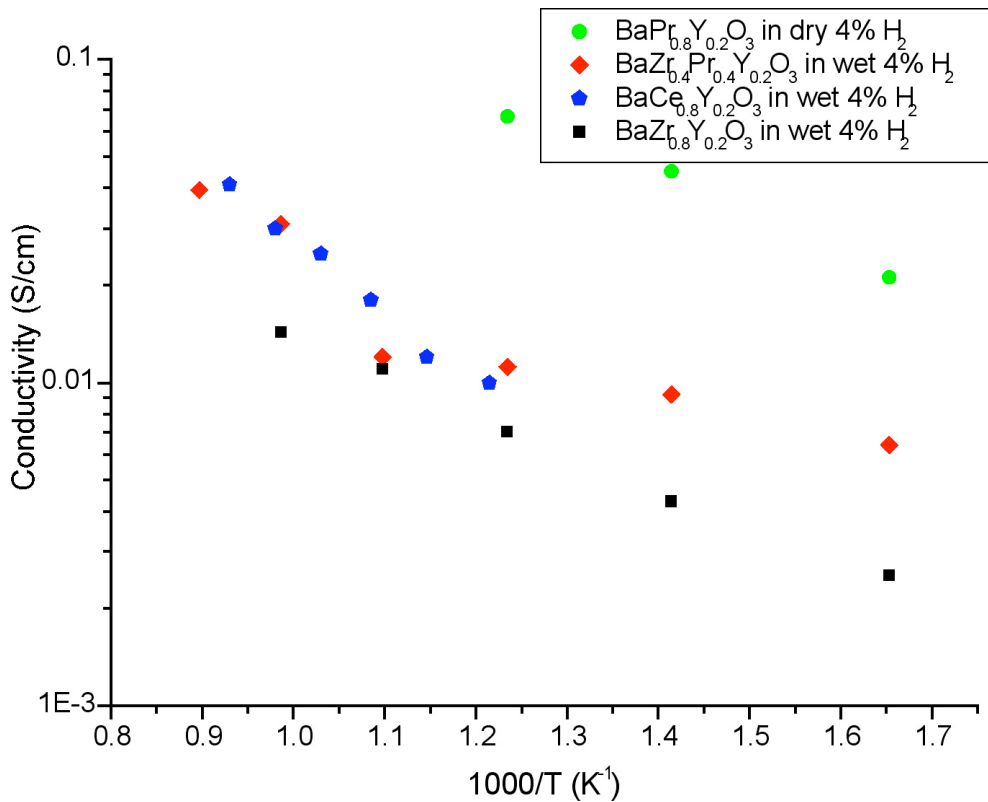


Figure 3. Bulk conductivity vs. inverse temperature for selected compositions in the $\text{BaZr}_{0.8-x}\text{Pr}_x\text{Y}_{0.2}\text{O}_3$ system ($\text{BaCe}_{0.8}\text{Y}_{0.2}\text{O}_3$ included for comparison). Measurements for $\text{BaPr}_{0.8}\text{Y}_{0.2}\text{O}_3$ were made in dry 4% $\text{H}_2/\text{balance N}_2$ due to its poor stability in humid environments.

We next turn to the results from tests with ANL-3e membranes. Figure 4 shows that the hydrogen flux through a 22- μm -thick ANL-3e membrane increases linearly with the difference in the square root of the hydrogen partial pressure in the feed and sweep gases. This behavior is characteristic of bulk-limited hydrogen diffusion through a metal phase and is expected, because the membrane contains a hydrogen transport metal, and the ceramic phase has a low hydrogen permeability. Such behavior suggests that reducing the membrane thickness may increase the hydrogen flux.

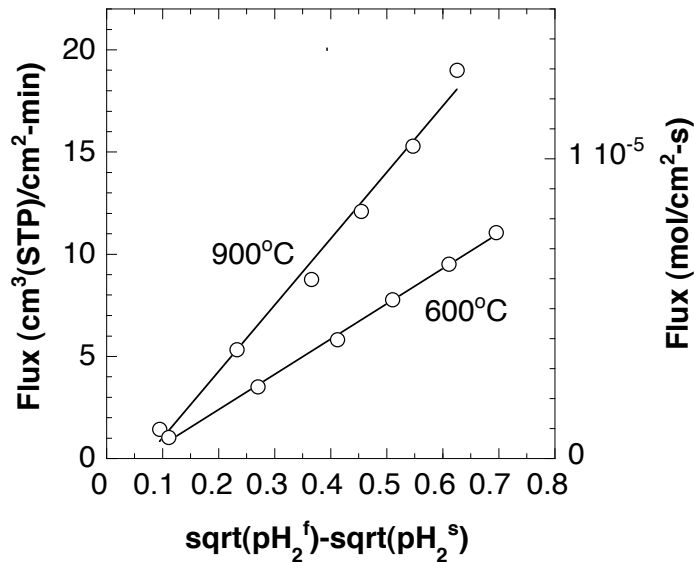


Figure 4. Hydrogen flux through 22- μm -thick ANL-3e membrane vs. difference in the square root of hydrogen partial pressure for the feed (pH_2^f) and sweep (pH_2^s) gases at 900 and 600°C.

Figure 5 shows the hydrogen flux of ANL-3e membranes versus the inverse of membrane thickness at 900°C using 100% H_2 as the feed gas. As with ANL-3a membranes made from the same hydrogen transport metal but a different ceramic matrix, the hydrogen flux of ANL-3e membranes varies linearly with the inverse of membrane thickness. This behavior indicates that the hydrogen permeation is controlled by bulk diffusion over this thickness range (22-100 μm). The highest flux for the ANL-3e membranes (19.0 $\text{cm}^3(\text{STP})/\text{min}\text{-cm}^2$) was only slightly lower than the record flux measured with an ANL-3a membrane (20 $\text{cm}^3(\text{STP})/\text{min}\text{-cm}^2$) [16]. However, if the ceramic phase merely supports the hydrogen transport metal and does not influence the hydrogen permeation, the ANL-3e membrane should have had the higher flux, because it was slightly thinner (22 μm vs. 40 μm) and contained an equal concentration (50 vol.%) of the same hydrogen transport metal. This apparent anomaly may suggest that the ceramic phase plays a secondary role in hydrogen permeation.

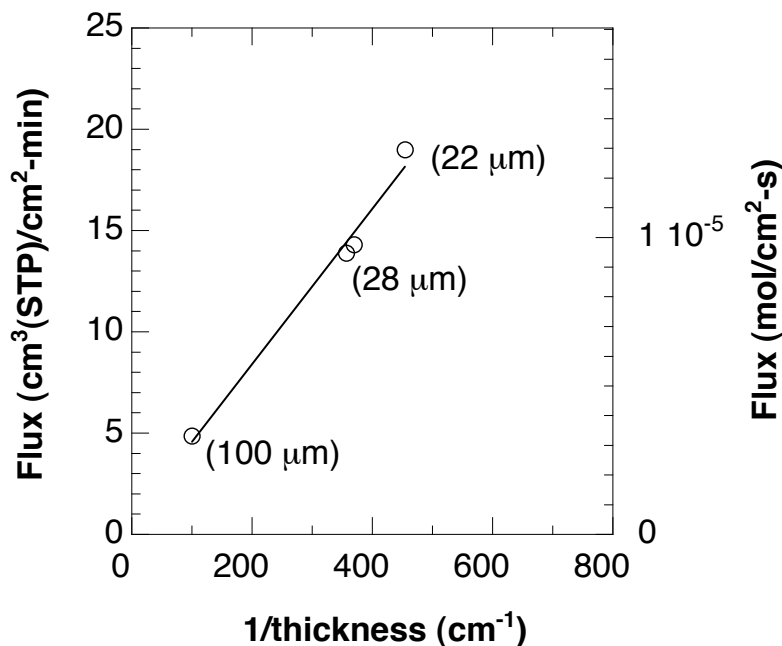


Figure 5. Hydrogen flux through ANL-3e membranes versus inverse of membrane thickness at 900°C using 100% H₂ as the feed gas.

Figure 6 shows the hydrogen flux of an ANL-3e membrane (thickness = 100 μm) versus time at several temperatures in feed gas of 51 ppm H₂S and 19.6% H₂/balance He. For the initial (time = 0 h) reading at each temperature, UHP H₂ and UHP He were mixed with mass flow controllers to give the same hydrogen concentration that the H₂S-containing gas would subsequently contain. After measurement of the initial hydrogen flux, UHP H₂ was switched to H₂ with 250 ppm H₂S to measure the flux versus time. At every temperature, the hydrogen flux decreased slightly during the first hour of exposure but was stable thereafter. At 900°C, the flux actually increased slightly during longer exposures, and the final flux was only ≈3% lower than the initial flux. The reason for the initial decrease in flux is not understood at this point, but thermodynamic data indicate that reaction between the hydrogen transport metal and H₂S is not favorable under these conditions.

Figure 7 shows the hydrogen flux of an ANL-3e membrane (thickness = 200 μm) versus time at 900°C in feed gases with different concentrations of H₂S. As in the earlier measurements with 51 ppm H₂S, a mixture of UHP H₂ and UHP He was used for the initial reading, then UHP H₂ was switched to an H₂S-containing gas. For measurements with a given H₂S concentration, the hydrogen concentration was constant during the initial and subsequent measurements. In the gas mixtures with 97 ppm H₂S (19.4% H₂) and 400 ppm H₂S (79.8% H₂), the hydrogen flux decreased moderately (~10%) in the first hour of exposure and then was stable, perhaps even increasing slightly with time.

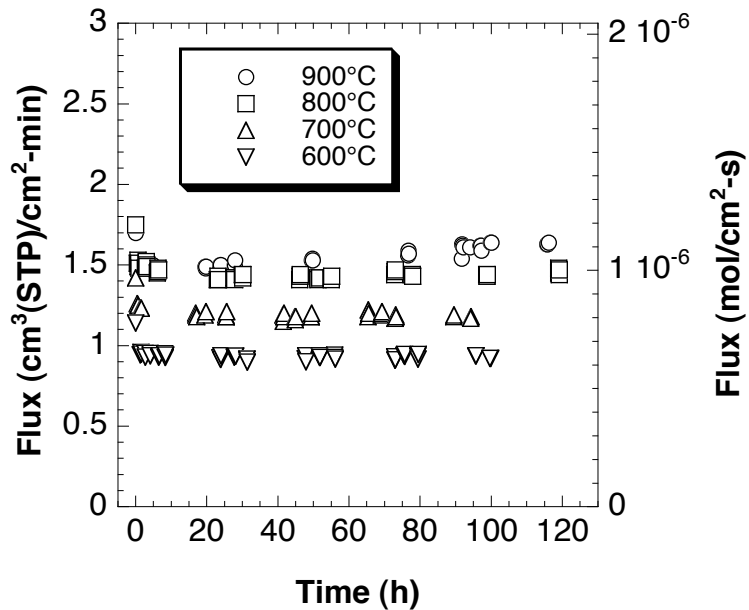


Figure 6. Hydrogen flux vs. time at several temperatures for 100- μ m-thick ANL-3e membrane in feed gas of 51 ppm H_2S /19.6% H_2 /balance He.

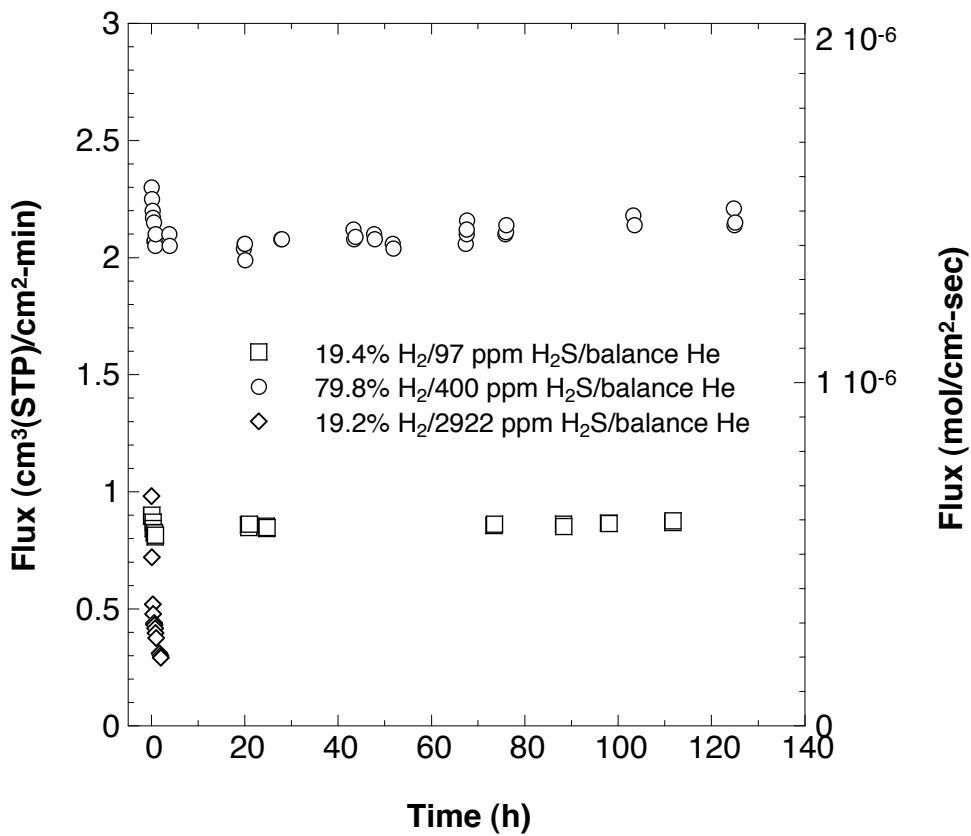


Figure 7. Hydrogen flux of 200- μ m-thick ANL-3e membrane at 900°C in feed gases with range of H_2S concentrations.

The hydrogen flux of the ANL-3e membrane decreased sharply after gas containing 2922 ppm H₂S (19.2% H₂) was introduced into the reactor. The flux decreased ≈60% during the first hour of exposure and ≈70% after 2 h of exposure and continued to decrease at longer exposures. In addition, leakage through the sample increased with time, as indicated by the measured He concentration in the sweep gas. After 70 h of exposure, the sample was cooled in He. Penetration of the sample by isopropyl alcohol, from one face to the other, showed that the sample contained interconnected porosity after the permeation test in 2922 ppm H₂S; alcohol had not penetrated the sample before the permeation test. Also, examination of the sample by scanning electron microscopy indicated a loss of metal from the membrane surface. These results suggest that the sharp drop in hydrogen flux and increase in leakage rate were caused by loss of the hydrogen transport metal. In combination with the results for lower H₂S concentrations, this finding indicates that the stability limit for ANL-3e membranes in H₂S-containing atmospheres is in the range of 400-2922 ppm H₂S.

CONCLUSIONS

We have developed various membranes that nongalvanically separate hydrogen from gas mixtures. To increase the hydrogen flux in some of these membranes, as well as improve their mechanical strength and thermodynamic stability, we are investigating the BaZr_{0.8-x}Pr_xY_{0.2}O₃ system as a possible alternative to BCY. While some compositions in the BaZr_{0.8-x}Pr_xY_{0.2}O₃ system exhibit promising conductivity, their stability remains an important issue.

The hydrogen flux through ANL-3e membranes increase linearly with the difference in the square root of hydrogen partial pressure for the feed and sweep gases and with the inverse of membrane thickness over the range 22-100 μm. This behavior indicates that the flux is limited by bulk diffusion of hydrogen in this thickness range. The highest measured hydrogen flux for an ANL-3e membrane (thickness ≈22 μm) was 19.0 cm³ (STP)/min-cm² at 900°C using 100% H₂ as the feed gas. This value is only slightly lower than the record flux measured with an ANL-3a membrane (20 cm³(STP)/min-cm²). The hydrogen flux of ANL-3e membranes was stable, after a small initial decrease, for up to 120 h in atmospheres containing up to 400 ppm H₂S. While long-term (>120 h) studies are required, these results indicate that the ANL membranes may be suitable for practical applications.

ACKNOWLEDGMENT

* This work was supported by U.S. Department of Energy, Office of Fossil Energy, National Energy Technology Laboratory's Gasification Technologies Program, under Contract W-31-109-Eng-38.

REFERENCES

- [1]. H. Iwahara, T. Yajima, and H. Uchida, *Solid State Ionics*, 70/71, 267 (1994).
- [2]. H. Iwahara, *Solid State Ionics*, 77, 289 (1995).
- [3]. J. Guan, S. E. Dorris, U. Balachandran, and M. Liu, *Solid State Ionics*, 100, 45 (1997).
- [4]. J. Guan, S. E. Dorris, U. Balachandran, and M. Liu, *J. Electrochem. Soc.*, 145, 1780 (1998).
- [5]. J. Guan, S. E. Dorris, U. Balachandran, and M. Liu, *Ceram. Trans.*, 92, 1 (1998).
- [6]. U. Balachandran, T. H. Lee, and S. E. Dorris, in *Proc. 16th Annual International Pittsburgh Coal Conf.*, Pittsburgh, PA, Oct. 11-15, 1999,
- [7]. U. Balachandran, T. H. Lee, G. Zhang, S. E. Dorris, K. S. Rothenberger, B. H. Howard, B. Morreale, A. V. Cugini, R. V. Siriwardane, J. A. Poston Jr., and E. P. Fisher, in *Proc. 26th Intl. Technical Conf. on Coal Utilization and Fuel Systems*, Clearwater, FL, Mar. 5-8, 2001, Coal Technical Association, Gaithersburg, MD, pp. 751-761.
- [8]. U. Balachandran, Argonne National Laboratory Proton-Conducting Membranes-Annual Report for FY 2001.
- [9]. T. Norby, *Solid State Ionics*, 125, 1 (1999).
- [10]. T. Fukui, S. Ohara, and S. Kawatsu, *Solid State Ionics*, 116, 331 (1999).
- [11]. T. Fukui, S. Ohara, and S. Kawatsu, *J. Power Sources*, 71, 164 (1998).
- [12]. K. D. Kreuer, *Solid State Ionics*, 125, 285 (1999).
- [13]. T. Schober and H. G. Bohn, *Solid State Ionics*, 127, 351 (2000).
- [14]. U. Balachandran, Argonne National Laboratory Proton-Conducting Membranes-Annual Report for FY2002.
- [15]. R. D. Shannon, *Acta Cryst.*, A32, 751 (1976).
- [16]. U. Balachandran, Argonne National Laboratory Proton-Conducting Membranes-Quarterly Report for October-December, 2002.